Sigma J Eng & Nat Sci 9 (2), 2018, 157-168

Publications Prepared for the 20. National Mechanics Congress

Research Article

THE DYNAMIC ANALYSIS OF A LINEAR VISCOELASTIC PLANAR ELLIPTICAL BEAM

Merve ERMİS*[1], Akif KUTLU[2], Nihal ERATLI[3], Mehmet Hakkı OMURTAG[4]

[1]*Istanbul Technical University, Dep. of Civil Eng., Maslak-ISTANBUL;* ORCID:0000-0003-0201-6586
[2]*Istanbul Technical University, Dep. of Civil Eng., Maslak-ISTANBUL;* ORCID:0000-0001-6865-3022
[3]*Istanbul Technical University, Dep. of Civil Eng., Maslak-ISTANBUL;* ORCID:0000-0003-3788-9870
[4]*Istanbul Technical University, Dep. of Civil Eng., Maslak-ISTANBUL;* ORCID:0000-0003-2669-6459

Received: 01.02.2018 Revised: 07.05.2018 Accepted: 23.07.2018

ABSTRACT

The objective of this study is to investigate the dynamic behaviour of a linear viscoelastic elliptical beam subjected to the vertical distributed loading by using the mixed finite method based on Timoshenko beam theory. It is assumed that, the linear viscoelastic material exhibits the standard type of distortional behaviour while having elastic Poisson's ratio. The finite element analysis is carried out in Laplace space, the material properties are implemented into the formulation through the use of the correspondence principle. The results are transformed back to the time domain numerically by using of the Modified Durbin's transformation algorithm. Through the analysis, two different types of impulsive load are considered, namely, isosceles triangular and right triangular impulsive load with the same duration and the maximum intensity of distributed load. A circular and two different elliptically oriented cross-sections are selected keeping the net cross-sectional areas equal to each other. The influence of different types of impulsive loads and cross-sections on the dynamic behaviour of viscoelastic elliptical planar beam with fixed-fixed boundary condition is investigated in detail and the examples are presented as original examples for the literature.
Keywords: Elliptical planar beam, viscoelastic material, dynamic analysis, impulsive load, mixed finite element method.

1. INTRODUCTION

Referring to the developing technology, curved beam elements are widely used in mechanical, civil, mechatronics and aerospace engineering as a structural construction member. They are used in advanced structures such as bridges, railways, aircrafts, turbine blades, connector elements and space vehicles. These needs are required to a wide range of curved element (elliptic, parabola, catenary, cycloid, and circle) having curvature range along the arc length with different section shapes and sizes. Due to internal friction, viscous effects are important on behaviour under dynamic and impulsive type loads *etc*, of some materials, such as polymers. Different viscoelastic mechanical models, such as the well-known Standard, Kelvin and Maxwell model *etc*, can simulate the viscous effects.

* Corresponding Author: e-mail: ermism@itu.edu.tr, tel: (212) 285 65 52

When elastic material is considered, there are numerous studies about static and dynamic analysis of elastic space (straight, curved planar and 3D) beams in the literature. Some of these works related to circular / non-circular planar curves can be given as follow: Static analysis is considered in [1] and [2]. Free vibration analysis are investigated in [3]-[9]. Dynamic analysis are studied without damping effect in [10]-[12], and, with damping effect in [13], respectively. When viscoelastic material is considered, there are many studies for linear viscoelastic straight beam in [14]- [20], whereas the studies about linear viscoelastic planar curved beams are limited for circular beam in [21]-[23], and, for non-circular beams in [24].

In this study, the dynamic analysis of a linear viscoelastic planar elliptical beam having three different cross-sections (circular cross-section, two different elliptically oriented cross-sections) are examined via mixed finite element method (MFEM) based on Timoshenko beam theory. By using the linear shape functions, the exact nodal arc length and curvature values are inserted into the finite element matrix [25]. The exact analytical expression of arc length and curvature of an elliptical plane curve is derived by using the formulation given in [26]. The analysis is performed in Laplace space by using the correspondence principle [27] and the results are transformed back to time domain numerically by Modified Durbin algorithm [28]-[30]. The mixed finite element algorithm used in this study was verified by Eratlı *et al.* 2014 [31], also used in [32] and [33]. Through the analysis, the viscoelastic model exhibits standard type of distortional behaviour while having elastic Poisson's ratio. The linear viscoelastic analysis of planar elliptical beam subjected to isosceles triangular and right triangular impulsive type of uniformly distributed load is performed. Beam is fixed at both ends. As far as the knowledge of the authors, this study is a new contribution to the literature with some benchmark examples.

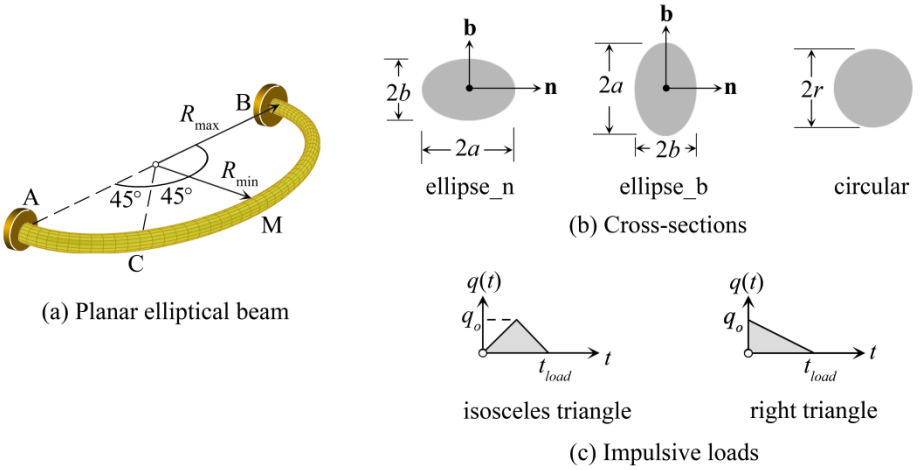

Figure 1. Planar elliptical beam having different cross-sections subjected to vertical distributed impulsive type dynamic load

2. FUNCTIONAL IN LAPLACE SPACE AND MIXED FE FORMULATION

Space Curve in Frenet Frame: A space curve is described by a position vector $\mathbf{R}(s)$, where s is the arc length parameter of the rod axis. The unit vectors of the Frenet Coordinate system can be given as: $\mathbf{t}(s)=\mathbf{R}_{,s}$, $\mathbf{n}(s)=\mathbf{R}_{,ss}/\left\|\mathbf{R}_{,ss}\right\|$, $\mathbf{b}(s)=\mathbf{t}(s)\times\mathbf{n}(s)$ where $\mathbf{t}$, $\mathbf{n}$ and $\mathbf{b}$ are the tangential, normal and binormal unit vectors, respectively. The differentiation with respect to arc length s is denoted by comma (*e.g.* $\mathrm{d}\mathbf{R}/\mathrm{d}s=\mathbf{R}_{,s}$). The differential relations between the unit vectors of

Frenet c oordinate are $\mathbf{t}(s)_{,s} = \chi(s)\mathbf{n}(s)$, $\mathbf{n}(s)_{,s} = \tau(s)\mathbf{b}(s) - \chi(s)\mathbf{t}(s)$, $\mathbf{b}(s)_{,s} = -\tau(s)\mathbf{n}(s)$ where $\chi(s) = \left\|\mathbf{R}_{,ss}\right\|$ and $\tau(s) = \mathbf{b}(s)\cdot\mathbf{n}(s)_{,s}$ represent the curvature and the torsion of the space curve [34], respectively. By choosing the position vector $\mathbf{R}(\varphi) = \{x(\varphi), y(\varphi), z(\varphi)\}$ in Cartesian coordinate system as a parametric function of horizontal angle φ, the differential relation between arc length s and the horizontal angle φ can be defined as $s_{,\varphi} = c(\varphi) = \left\|\mathbf{R}_{,\varphi}\right\|$ with $c(\varphi)$ being the gradient of arc length [26].

Plane Curve: A planar curve is described by a position vector $\mathbf{r}(\varphi)$, the analytical expressions for the curvature and the arc length in terms of position vector becomes $\chi^p(\varphi) = \left\|\mathbf{r}_{,ss}\right\|$, $c^p(\varphi) = \left\|\mathbf{r}_{,\varphi}\right\|$, $s^p_{,\varphi} = c^p(\varphi)$. We note that the superscript " p " is used to denote that these quantities are written for a plane curve. For a planar elliptical curve shown in Fig.1a, $x(\varphi) = R_{\max}\cos\varphi$, $y(\varphi) = R_{\min}\sin\varphi$ where $R_{\min}$ and $R_{\max}$ are the minimum and maximum radius, respectively.

Viscoelastic Material Model: In this study, the viscoelastic material exhibits the standard type of distortional behaviour while having elastic Poisson's ratio, and the complex shear modulus can be expressed as given in [35] and [36]: $\bar{G} = G\left(1+\beta^G\tau_r^G z\right)/\left(1+\tau_r^G z\right)$; $\beta^G = G_g/G > 1$ where τ_r^G is the retardation time, G is the equilibrium value of shear modulus and G_g is the instantaneous value of relaxation function associated with shear modulus.

Field Equations: The field equations for a space rod are based on Timoshenko beam theory. The associated functional in Laplace transformed space is given by:

$$\left.\begin{aligned}\bar{\mathbf{I}}(\bar{\mathbf{y}}) = &-[\bar{\mathbf{u}},\bar{\mathbf{T}}_{,s}] + [\mathbf{t}\times\bar{\mathbf{\Omega}},\bar{\mathbf{T}}] - [\bar{\mathbf{M}}_{,s},\bar{\mathbf{\Omega}}] - \tfrac{1}{2}[\mathbf{C}_\kappa\bar{\mathbf{M}},\bar{\mathbf{M}}] - \tfrac{1}{2}[\mathbf{C}_\gamma\bar{\mathbf{T}},\bar{\mathbf{T}}] + \tfrac{1}{2}\rho A z^2\left[\bar{\mathbf{u}},\bar{\mathbf{u}}\right]\\ &+ \tfrac{1}{2}\rho\, z^2\left[\mathbf{I}\bar{\mathbf{\Omega}},\bar{\mathbf{\Omega}}\right] - \left[\bar{\mathbf{q}},\bar{\mathbf{u}}\right] - \left[\bar{\mathbf{m}},\bar{\mathbf{\Omega}}\right] + [(\bar{\mathbf{T}}-\hat{\bar{\mathbf{T}}}),\bar{\mathbf{u}}]_\sigma + [(\bar{\mathbf{M}}-\hat{\bar{\mathbf{M}}}),\bar{\mathbf{\Omega}}]_\sigma + [\hat{\bar{\mathbf{u}}},\bar{\mathbf{T}}]_\varepsilon + [\hat{\bar{\mathbf{\Omega}}},\bar{\mathbf{M}}]_\varepsilon\end{aligned}\right\} \quad (1)$$

In Eq. (1), the Laplace transformed variables are denoted by the over bars; z is the Laplace transformation parameter; $\bar{\mathbf{u}}(\bar{u}_t, \bar{u}_n, \bar{u}_b)$, $\bar{\mathbf{\Omega}}(\bar{\Omega}_t, \bar{\Omega}_n, \bar{\Omega}_b)$, $\bar{\mathbf{T}}(\bar{T}_t, \bar{T}_n, \bar{T}_b)$ and $\bar{\mathbf{M}}(\bar{M}_t, \bar{M}_n, \bar{M}_b)$ are the displacement, rotation, force and moments vectors, respectively (given in terms of Frenet frame components). $\bar{\mathbf{q}}$ and $\bar{\mathbf{m}}$ are the distributed external force and moment vectors, respectively. $\bar{\mathbf{C}}_\gamma$ and $\bar{\mathbf{C}}_\kappa$ are the compliance matrices. ρ is the density of homogenous material, A is the area of cross-section and $\mathbf{I}(I_t, I_n, I_b)$ is the moment of inertia vector. In the mixed finite element formulation, a two noded curvilinear element is used to discretize the domain of the planar curved beam. The derivation procedure of a functional Eq. (1), exists in [31], is based on Gâteaux differentiation and potential operator concept [37]-[39] .

3. NUMERICAL EXAMPLES

Common parameters: Through the analysis, geometric parameters of elliptical beam and cross-sections are taken as follows: the minimum radius of elliptical beam to the maximum radius of elliptical beam ratio $R_{\min}/R_{\max} = 0.5$ where $R_{\max} = 1\text{m}$; a circular and two elliptical cross-section having different orientations are used in the analysis. The orientations of the two different elliptical cross-sections are as shown in Fig.1b. The abbreviations "ellipse_n" and "ellipse_b" are used to denote, respectively, the elliptical cross-sections having major axis oriented horizontal and vertical. The cross sectional areas of the circular and the two elliptical sections are taken the

same. The dimensions of the elliptical and circular cross-sections are $a = 5\text{cm}$, $b = 2.5\text{cm}$ and $r = 3.53553\text{cm}$. The beam is fixed at both ends. Torsional moment of inertia for an elliptical cross-section is calculated by using the equation $I_t = \left(\pi a^3 b^3\right) / \left(a^2 + b^2\right)$ [40].

A convergence and verification example for elastic analysis: *A* convergence analysis is performed over the natural frequencies of the planar elliptical beam having the circular, elliptical_n and elliptical_b cross-sections and verified with the solutions of SAP2000 in [41].

Viscoelastic analysis: The material parameters are the shear modulus $G = 7 \times 10^5\,\text{Pa}$, Poisson's ratio $\upsilon = 0.3$, the density of material $\rho = 7850\,\text{kg/m}^3$, the retardation time $\tau_r^G = 0.05\text{s}$ and the ratio $\beta^G = 1.5$. By using the parameters τ_r^G, β^G and G, the complex shear modulus $\bar{G}$ is determined. The quasi-static and dynamic responses of the beam which is subjected to a vertical distributed dynamic load $q = q_z(t)$ are investigated within $0 \le t \le 100\text{s}$. Isosceles triangular and right triangular impulsive type loads are used (Fig.1c). The area of the forced vibration zone of these loads is kept constant, the duration of load is $t_{load} = 40\text{s}$ and the maximum intensity of distributed load is $q_o = 10^{-3}\,\text{N/m}$. The analyses are carried out in Laplace transform space and the results are transformed back to time domain numerically by Modified Durbin algorithm [28]-[30]. For the inverse Laplace transformation algorithm, $N = 2^{11}$ and $aT = 6$ are used [31]. The vertical displacements $u_b^{\text{M}}(t)$ at the midpoint M, the rotations $\Omega_n^{\text{C}}(t)$ at point C, the forces $T_b^{\text{A}}(t)$ and the moments $M_t^{\text{A}}(t)$ and $M_n^{\text{A}}(t)$ at point A of the elliptical beam (Fig.1a) are investigated within time interval $0 \le t \le 100\text{s}$. For points A, C and M see Fig. 1a.

A convergence example for viscoelastic analysis: A convergence analysis of the planar elliptical beam having circular cross-section is carried out for 16, 24, 32, 40 and 48 elements. The first extremum peak values of the time histories of $u_b^{\text{M}}(t)$, $\Omega_n^{\text{C}}(t)$, $T_b^{\text{A}}(t)$, $M_t^{\text{A}}(t)$ and $M_n^{\text{A}}(t)$ for the isosceles triangular and the right triangular impulsive loads are tabulated in Tables 1-2, respectively. The results ($u_b^{\text{M}}(t)$, $\Omega_n^{\text{C}}(t)$, $T_b^{\text{A}}(t)$, $M_t^{\text{A}}(t)$ and $M_n^{\text{A}}(t)$) obtained by using 40 elements are normalized with respect to the results of 48 elements and percent differences are also given in Tables 1-2. In the following examples, 40 elements are employed.

Table 1. The convergence analysis for the isosceles triangular impulsive load. (n_e : number of element)

n_e	the first peak of the dynamic behaviour of elliptical beam having circular cross-section				
	$u_b^{\text{M}} \times 10^{-3}$ (mm)	$\Omega_n^{\text{C}} \times 10^{-6}$ (rad)	$T_b^{\text{A}} \times 10^{-4}$ (N)	$M_t^{\text{A}} \times 10^{-2}$ (N.mm)	$M_n^{\text{A}} \times 10^{-2}$ (N.mm)
16	-47.65	61.81	-12.10	-29.71	44.05
24	-47.34	60.86	-12.09	-29.94	43.25
32	-47.24	60.54	-12.09	-30.01	43.00
40	-47.19	60.38	-12.09	-30.04	42.88
48	-47.17	60.25	-12.09	-30.06	42.82
%diff.	-0.04	-0.22	0.00	0.07	-0.14

$\text{diff.\%} = \left(1 - \Delta_{40\text{el}} / \Delta_{48\text{el}}\right) \times 100$, Δ : u_b^{M} , Ω_n^{C} , T_b^{A} , M_t^{A} , M_n^{A}

Table 2. The convergence analysis for the right triangular impulsive load. (n_e : number of element)

n_e	the first peak of the dynamic behaviour of elliptical beam having circular cross-section				
	$u_b^{\mathrm{M}} \times 10^{-3}$ (mm)	$\Omega_n^{\mathrm{C}} \times 10^{-6}$ (rad)	$T_b^{\mathrm{A}} \times 10^{-4}$ (N)	$M_t^{\mathrm{A}} \times 10^{-2}$ (N.mm)	$M_n^{\mathrm{A}} \times 10^{-2}$ (N.mm)
16	-90.02	116.57	-19.67	-54.96	78.62
24	-89.51	114.82	-19.68	-55.33	77.10
32	-89.33	114.23	-19.68	-55.45	76.63
40	-89.24	113.96	-19.68	-55.50	76.42
48	-89.20	113.82	-19.68	-55.53	76.30
%diff.	-0.04	-0.13	0.00	0.05	-0.16

$\mathrm{diff.\%} = \left(1 - \Delta_{40\mathrm{el}} / \Delta_{48\mathrm{el}}\right) \times 100$, Δ : u_b^{M} , Ω_n^{C} , T_b^{A} , M_t^{A} , M_n^{A}

The effect of the dynamic impulsive load: The time history of $u_b^{\mathrm{M}}(t)$ of the planar elliptical beam having circular cross-section are given for isosceles triangular and right triangular impulsive type loads in Fig.2. The dynamic behaviour of the viscoelastic elliptical beam dissipates within the sampling time interval and approaches to the quasi-static case (see Fig.2). Under the same damping parameters, the behaviour of the viscoelastic case is oscillating close around the quasi-static case results for the impulsive isosceles triangular loading whereas it is not the case for impulsive right triangular case. The first extremum peak of $u_b^{\mathrm{M}}(t)$ belonging to the isosceles triangular impulsive load case are normalized with respect to the first extremum peak of $u_b^{\mathrm{M}}(t)$ belonging to the right triangular impulsive load for dynamic and quasi static cases, and, these percent differences are 47.12%, and -0.89%, respectively.

The effect of the cross-section: The dynamic behaviour of viscoelastic elliptical beams having three different cross-sectional geometries are compared with each other for isosceles triangular and right triangular impulsive type loads. For this purpose, circular, ellipse_n and ellipse_b cross-sections are considered. The time histories of $u_b^{\mathrm{M}}(t)$, $\Omega_n^{\mathrm{C}}(t)$, $T_b^{\mathrm{A}}(t)$, $M_t^{\mathrm{A}}(t)$ and $M_n^{\mathrm{A}}(t)$ are given in Figs.3 and 4. For points A, C and M see Fig. 1a. It is seen that; the time histories are significantly affected from the shape of the cross-section. Figs.3 and 4 may be discussed within the two time intervals namely, $0\mathrm{s} \le t \le 40\mathrm{s}$ and $40\mathrm{s} \le t \le 100\mathrm{s}$. In this case:

- For the forced vibration zone ($0\mathrm{s} \le t \le 40\mathrm{s}$), the first extremum peaks of $u_b^{\mathrm{M}}(t)$, $\Omega_n^{\mathrm{C}}(t)$, $T_b^{\mathrm{A}}(t)$, $M_t^{\mathrm{A}}(t)$ and $M_n^{\mathrm{A}}(t)$ of the isosceles triangular impulsive load are normalized with respect to the first extremum peaks of $u_b^{\mathrm{M}}(t)$, $\Omega_n^{\mathrm{C}}(t)$, $T_b^{\mathrm{A}}(t)$, $M_t^{\mathrm{A}}(t)$ and $M_n^{\mathrm{A}}(t)$ of the right triangular impulsive load for each type of cross-sections:

  - *In elips_b cross-section*: The percent reductions in the amplitude of $u_b^{\mathrm{M}}(t)$, $\Omega_n^{\mathrm{C}}(t)$, $T_b^{\mathrm{A}}(t)$, $M_t^{\mathrm{A}}(t)$ and $M_n^{\mathrm{A}}(t)$ are 47.1%, 47.0%, 38.6%, 45.9%, 43.9%, respectively.
  - *In circular cross-section*: The percent reductions in the amplitude of $u_b^{\mathrm{M}}(t)$, $\Omega_n^{\mathrm{C}}(t)$, $T_b^{\mathrm{A}}(t)$, $M_t^{\mathrm{A}}(t)$ and $M_n^{\mathrm{A}}(t)$ are 46.2%, 46.0%, 36.6%, 44.5%, 42.1%, respectively.
  - *In elips_n cros-section*: The percent reductions in the amplitude of $u_b^{\mathrm{M}}(t)$, $\Omega_n^{\mathrm{C}}(t)$, $T_b^{\mathrm{A}}(t)$, $M_t^{\mathrm{A}}(t)$ and $M_n^{\mathrm{A}}(t)$ are 46.1%, 46.1 %, 39.8%, 45.3% , 43.9%, respectively.

- For the free vibration zone ($40\text{s} \le t \le 100\text{s}$), the dynamic response of $u_b^{\mathrm{M}}(t)$, $\Omega_n^{\mathrm{C}}(t)$, $T_b^{\mathrm{A}}(t)$, $M_t^{\mathrm{A}}(t)$ and $M_n^{\mathrm{A}}(t)$ oscillates around zero along the free vibration zone with decreasing amplitude for both types of impulsive loads. The reduction in the amplitudes of these responses are more influential in the case of isosceles triangular impulsive type of loading. The responses determined for circular and ellipse_b cross-sections damp rapidly when compared with the ellipse_n.

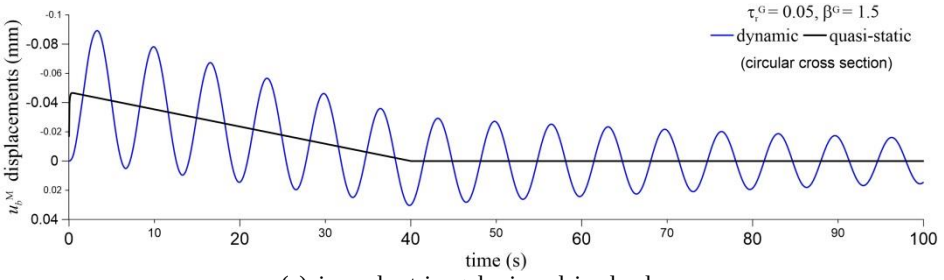

(a) isosceles triangular impulsive load.

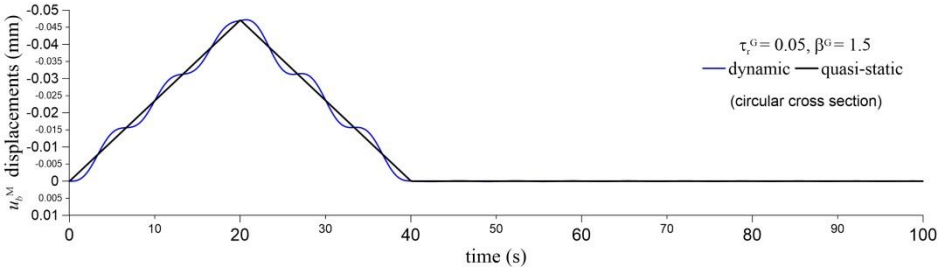

(b) right triangular impulsive load

Figure 2. The vertical displacements $u_b^{\mathrm{M}}(t)$ of the elliptical beam having circular cross-sections

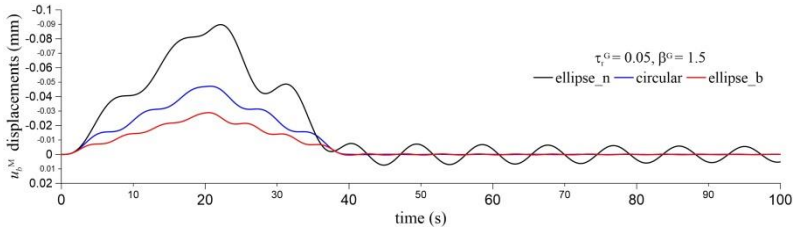

(a) the vertical displacements $u_b^{\mathrm{M}}(t)$

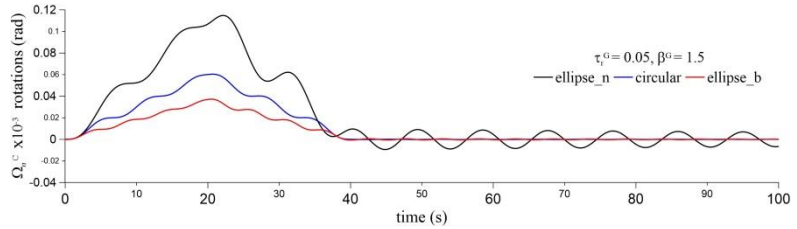

(b) the rotations $\Omega_n^{\mathrm{C}}(t)$

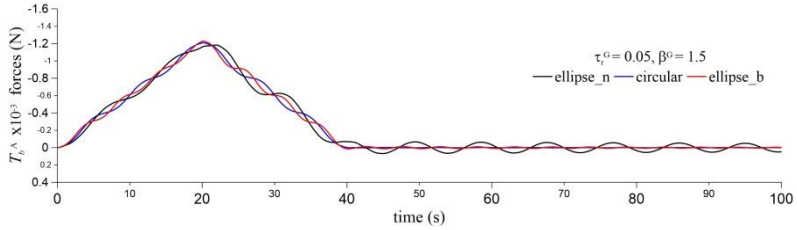

(c) the forces $T_b^{\mathrm{A}}(t)$

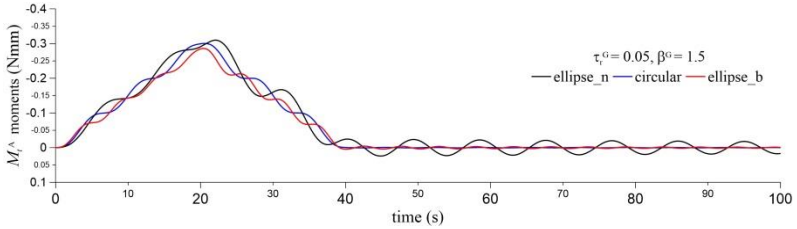

(d) the moments $M_t^{\mathrm{A}}(t)$

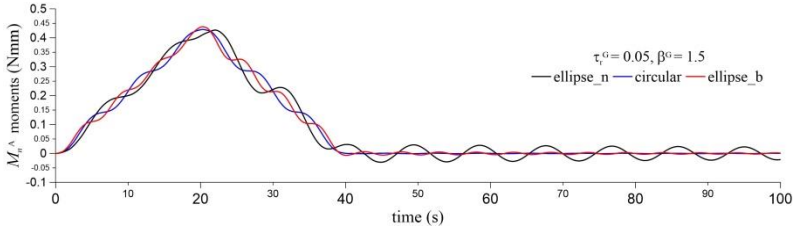

(e) the moments $M_n^{\mathrm{A}}(t)$

Figure 3. Time histories of the planar elliptical beam having cross-sections (circular, elips_n, and elips_b) subjected to isosceles triangular impulsive load.

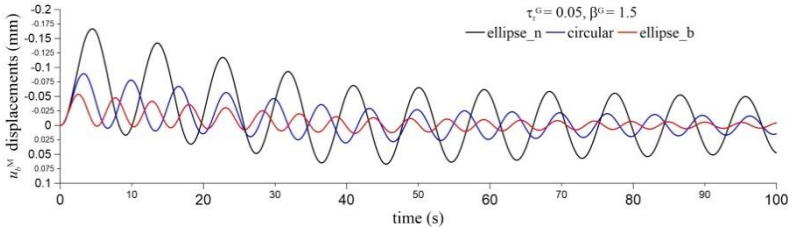

(a) the vertical displacements $u_b^{\mathrm{M}}(t)$

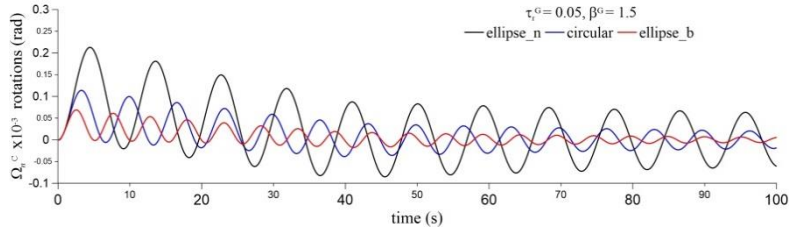

(b) the rotations $\Omega_n^{\mathrm{C}}(t)$

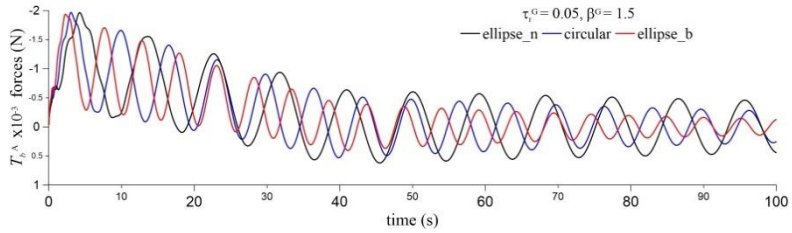

(c) the forces $T_b^{\mathrm{A}}(t)$

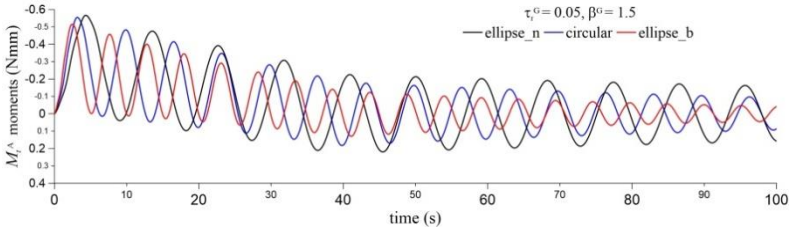

(d) the moments $M_t^{\mathrm{A}}(t)$

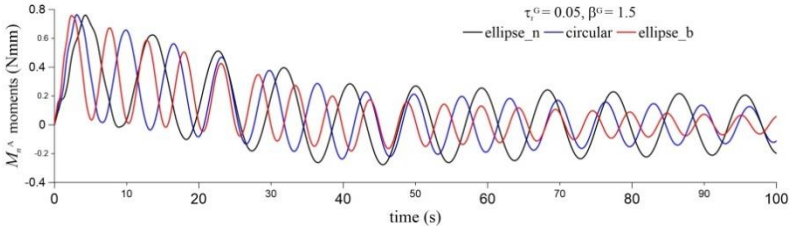

(e) the moments $M_n^{\mathrm{A}}(t)$

Figure 4. Time histories of the planar elliptical beam having cross-sections (circular, elips_n, and elips_b) subjected to right triangular impulsive load.

4. CONCLUSION

The dynamic viscoelastic response of the planar elliptical beam having a circular and two elliptical cross-sections with different orientations are analysed by using mixed FEM. For this purpose, the viscoelastic material behaviour is simulated by using the standard model and viscoelastic properties are accounted using the correspondence principle. The finite element solutions are carried out in the Laplace space. The results obtained in frequency domain are transformed back to time domain using modified Durbin's algorithm.

The effect of the cross-section on the time histories of the variables are:

- The vibration periods of $u_b^{\mathrm{M}}(t)$, $\Omega_n^{\mathrm{C}}(t)$, $T_b^{\mathrm{A}}(t)$, $M_t^{\mathrm{A}}(t)$ and $M_n^{\mathrm{A}}(t)$ for the beam having ellipse_n cross-section is the largest compared to the other two cross-sections.
- The first extremum peaks of $u_b^{\mathrm{M}}(t)$, $\Omega_n^{\mathrm{C}}(t)$ and $M_t^{\mathrm{A}}(t)$ for the beam having ellipse_n cross-section is the largest when compared with those obtained for the other two cross-sections.
- The difference between the first extremum of the time histories of $T_b^{\mathrm{A}}(t)$ are insignificant for the three cross-sectional geometries used in this study. This judgement is also valid for the time histories of $M_n^{\mathrm{A}}(t)$.
- The first extremum peaks of $u_b^{\mathrm{M}}(t)$ and $\Omega_n^{\mathrm{C}}(t)$ for circular and ellipse_b cross-section are normalized with respect to the first extremum peaks of $u_b^{\mathrm{M}}(t)$ and $\Omega_n^{\mathrm{C}}(t)$ of the ellipse_n cross-section. The discussion is as follows:
  - *In isosceles triangular impulsive load:* The percent reductions in the amplitudes of $u_b^{\mathrm{M}}(t)$ and $\Omega_n^{\mathrm{C}}(t)$ are 47.4 % and 47.4% for the beam having circular cross-section, and, 67.8% and 68.5% for the beam having ellipse_b cross-section, respectively.
  - *In right triangular impulsive load*: The percent reductions in the amplitudes of $u_b^{\mathrm{M}}(t)$ and $\Omega_n^{\mathrm{C}}(t)$ are 46.4% and 46.5% for the beam having circular cross-section, and, 67.8% and 67.6% for the beam having ellipse_b cross-section, respectively.

The effect of the impulsive load type on the time histories of the variables are:

- If the first extremum peaks of the time histories of the quasi-static case for the isosceles triangular and right triangular impulsive loads (see Fig.2) are normalized with respect to the first extremum peaks of the corresponding dynamic loading cases, the percent reductions are obtained as 0.39%, 47.79%, respectively.
- The results show that, the dynamic behaviour of the linear viscoelastic planar elliptical beam is affected from the form of applied dynamic loading, although the forced vibration areas and the duration of loading are the same. As a result, the type of cross-section and loading to be used in special problems must be carefully selected.

As far as the knowledge of the authors, the linear viscoelastic elliptical beam analysis using mixed FEM is an original example.

REFERENCES

[1] F.N. Gimena, P. Gonzaga, L. Gimena (2008). Stiffness and transfer matrices of a non-naturally curved 3D-beam element. *Engineering Structures* 30(6), pp. 1770-1781.

[2] E. Tufekci, U. Eroglu, S.A. Aya (2017). A new two-noded curved beam finite element formulation based on exact solution, *Engineering with Computers* 33(2), pp. 261-273.

[3] C.S. Huang, Y.P. Tseng, A.W. Leissa, K.Y. Nieh (1998a). An exact solution for in-plane vibrations of an arch having variable curvature and cross section, *International Journal of Mechanical Sciences* 40(11), pp. 1159-1173.

[4] S.J. Oh, B.K. Lee, I.W. Lee (1999). Natural frequencies of non-circular arches with rotatory inertia and shear deformation, *Journal of Sound and Vibration*, 219(1), pp. 23-33.

[5] S.J. Oh, B.K. Lee, I.W. Lee (2000). Free vibration of non-circular arches with non-uniform cross-section. *International Journal of Solids and Structures* 37, pp. 4871-4891.

[6] F. Yang, R. Sedaghati, E. Esmailzadeh (2008). Free in-plane vibration of general curved beams using finite element method, *Journal of Sound and Vibration* 318, pp. 850-867.

[7] A. Shahba, R. Attarnejad, S.J. Semnani, H.H. Gheitanbaf (2013). New shape functions for non-uniform curved Timoshenko beams with arbitrarily varying curvature using basic displacement functions, *Meccanica* 48(1), pp. 159-174.

[8] A.T. Luu, N.I. Kim, J. Lee (2015). Isogeometric vibration analysis of free-form Timoshenko curved beams. *Meccanica* 50(1), pp.169-187.

[9] B.K. Lee, K.K. Park, S.J. Oh, T.E. Lee (2016). Planar free vibrations of horseshoe elliptic arch. *KSCE Journal of Civil Engineering* 20(4), pp. 1411-1418.

[10] Y. Tene, M. Epstein, I. Sheinman (1975). Dynamics of curved beams involving shear deformation, *International Journal of Solids and Structures*, 11(7-8), 827-840.

[11] C.S. Huang, Y.P. Tseng, S.H. Chang (1998b). Out-of-plane dynamic responses of noncircular curved beams by numerical Laplace transform, *Journal of Sound and Vibration* 215(3), pp. 407–424.

[12] C.S. Huang, Y.P. Tseng, S.H. Chang, C.L. Hung (2000). Out-of-plane dynamic analysis of beams with arbitrarily varying curvature and cross-section by dynamic stiffness matrix method. *International Journal of Solids and Structures* 37(3), pp. 495-513.

[13] C.S. Huang, Y.P. Tseng, C.R. Lin (1998c). In-plane transient responses of an arch with variable curvature using the dynamic stiffness method with numerical Laplace transform, *Journal of Engineering Mechanics* ASCE 124(8), pp. 826–835.

[14] Y. Yamada, H. Takabatake and T. Sato (1974). Effect of time-dependent material properties on dynamic response, *International Journal for Numerical Methods in Engineering*, 8, pp. 403–414. doi: 10.1002/nme.1620080216.

[15] T.M. Chen (1995). The hybrid Laplace transform/finite element method applied to the quasi-static and dynamic analysis of viscoelastic Timoshenko beams, *International Journal for Numerical Methods in Engineering*, 38, pp. 509–522. doi: 10.1002/nme.1620380310.

[16] C.M. Wang, T.Q. Yang and K.Y. Lam (1997). Viscoelastic Timoshenko beam solutions from Euler-Bernoulli solutions, *Journal of Engineering Mechanics* – ASCE, 123, pp. 746–748. doi: 10.1061/(ASCE)0733-9399(1997)123:7(746).

[17] T. Kocatürk, M. Şimşek (2006a). Dynamic analysis of eccentrically prestressed viscoelastic Timoshenko beams under a moving harmonic load, *Computers and Structures*, 84, pp. 2113–2127. doi: 10.1016/j.compstruc.2006.08.062.

[18] T. Kocatürk, M. Şimşek (2006b). Vibration of viscoelastic beams subjected to an eccentric compressive force and a concentrated moving harmonic force, *Journal of Sound and Vibration*, 291, pp. 302–322. doi: 10.1016/j.jsv.2005.06.024.

[19] A. Keramat and K.H. Shirazi (2014). Finite element based dynamic analysis of viscoelastic solids using the approximation of Volterra integrals, *Finite Elements in Analysis and Design*. 86, pp. 89-100. doi: 10.1016/j.finel.2014.03.010.

[20] O. Martin (2016). A modified variational iteration method for the analysis of viscoelastic beams, *Applied Mathematical Modelling*, 40, pp. 7988–7995. doi: 10.1016/j.apm.2016.04.011.

[21] I. Granstam (1973). Contact between a curved viscoelastic beam and a rigid plane, *The Journal of Strain Analysis for Engineering Design*, 8, pp. 58–64. doi:10.1243/03093247V081058.

[22] K. Nagaya, Y. Hirano (1977). In-Plane Vibration of Viscoelastic Circular Rod with Consideration of Shearing Deformation and Rotatory Inertia, *Bulletin of JSME*, 20, pp. 539-547. doi:10.1299/jsme1958.20.539.

[23] A.R. Noori, T. A. Aslan, B. Temel (2018). Damped transient response of in-plane and out-of-plane loaded stepped curved rods, B. *J Braz. Soc. Mech. Sci. Eng.*, 40,28. https://doi.org/10.1007/s40430-017-0949-8

[24] T. Irie T, G. Yamada and I. Takahashi (1980). The steady state out-of-plane response of a Timoshenko curved beam with internal damping. *Journal of Sound and Vibration* 71(1), pp. 145-156.

[25] M.H. Omurtag and A.Y. Aköz (1992a). The mixed finite element solution of helical beams with variable cross-section under arbitrary loading. *Computers and Structures* ,43(2), pp.325-331.

[26] M. Ermis and M.H. Omurtag (2017). Static and Dynamic Analysis of Conical Helices Based on Exact Geometry via Mixed FEM, *International Journal of Mechanical Sciences*, 131-132, pp. 296-304. doi: 10.1016/j.ijmecsci.2017.07.010

[27] I.R. Shames, F.A. Cozarelli, *Elastic and Inelastic Stress Analysis*, CRC Press Inc., 1997.

[28] H. Dubner and J. Abate (1968). Numerical inversion of Laplace transforms by relating them to the finite Fourier cosine transform, *Journal of the ACM*. 15 115–123. doi: 10.1145/321439.321446

[29] F. Durbin (1974). Numerical inversion of Laplace transforms: An efficient improvement to Dubner and Abate's method, *Computer Journal*, 17, pp. 371–376. doi: 10.1093/comjnl/17.4.371

[30] G. Narayanan, Numerical *Operational Methods in Structural Dynamics*, Doktora Tezi, University of Minnesota, 1980.

[31] N. Eratlı, H. Argeso, F.F. Çalım, B. Temel and M.H. Omurtag (2014). Dynamic analysis of linear viscoelastic cylindrical and conical helicoidal rods using the mixed FEM, Journal *of Sound and Vibration,* 333, pp. 3671–3690.

[32] M. Ermiş, N. Eratlı and M.H. Omurtag (2015). The influence of the rotary inertia on the dynamic behavior of viscoelastic non-cylindrical helicoidal bars, *In AIP Conference Proceedings*, 1702(1), p. 190006. AIP Publishing. doi: 10.1063/1.4938973

[33] M. Ermis, N. Eratlı, H. Argeso, A. Kutlu, M.H. Omurtag. (2016) Parametric analysis of viscoelastic hyperboloidal helical rod, *Advances in Structural Engineering*, 19(9), pp.1420-1434. doi: 10.1177/1369433216643584.

[34] Struik DJ. Lectures on Classical Differential Geometry. New-York: Dover; 1988.

[35] Y. Mengi and H. Argeso (2006). A unified approach for the formulation of interaction problems by the boundary element method, *International Journal for Numerical Methods in Engineering*, 66, pp. 816-842. doi: 10.1002/nme.1585

[36] B. Baranoglu and Y. Mengi (2006). The use of dual reciprocity boundary element method in coupled thermoviscoelasticity, *Computer Methods in Applied Mechanics and Engineering*, 196, pp. 379-392. doi: 10.1016/j.cma.2006.07.003

[37] M.H. Omurtag, and A.Y. Aköz (1992b). Mixed finite element formulation of eccentrically stiffened cylindrical shells, *Computers and Structures,* 42(5), pp. 751-768.

[38] M.H. Omurtag, A.Y. Aköz (1993). A compatible cylindrical shell element for stiffened cylindrical shells in a mixed finite element formulation. *Computers and Structures,* 49(2), pp. 363-370.

[39] M.H. Omurtag, A.Y. Aköz (1994). Hyperbolic paraboloid shell analysis via mixed finite element formulation. *International journal for numerical methods in engineering*, 37(18), pp. 3037-3056.

[40] S. Timoshenko and J.N. Goodier, *Theory of elasticity*, McGraw-Hill, New York, 1951.
[41] M. Ermiş, A. Kutlu, N. Eratlı and M.H. Omurtag (2017). Viskoelastik eliptik düzlem çubukların dinamik analizi, XX th National Mechanics Congress, Uludağ University-Bursa, 05-09 September, 2017 (in Turkish). ISBN 978-975561491-5, pp.147-156.